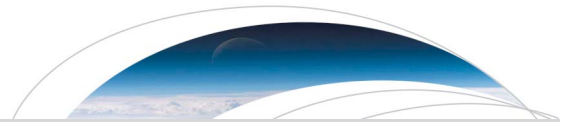




Originally published as:

Scheingross, J., Lo, D. Y., Lamb, M. P. (2017): Self-formed waterfall plunge pools in homogeneous rock. - *Geophysical Research Letters*, 44, 1, pp. 200—208.

DOI: <http://doi.org/10.1002/2016GL071730>



RESEARCH LETTER

10.1002/2016GL071730

Key Points:

- Experimental plunge pool formation is controlled by abrasion and sediment transport
- Vertical incision in plunge pools outpaces undercutting by an average of tenfold
- Upstream waterfall propagation in homogeneous rock is likely driven by vertical pool drilling

Supporting Information:

- Supporting Information S1

Correspondence to:

J. S. Scheingross,
joel.scheingross@gfz-potsdam.de

Citation:

Scheingross, J. S., D. Y. Lo, and M. P. Lamb (2017), Self-formed waterfall plunge pools in homogeneous rock, *Geophys. Res. Lett.*, *44*, 200–208, doi:10.1002/2016GL071730.

Received 25 OCT 2016

Accepted 29 NOV 2016

Accepted article online 4 DEC 2016

Published online 13 JAN 2017

Self-formed waterfall plunge pools in homogeneous rock

Joel S. Scheingross^{1,2} , Daniel Y. Lo¹ , and Michael P. Lamb¹ 

¹Division of Geological and Planetary Sciences, California Institute of Technology, Pasadena, California, USA, ²Now at Helmholtz Centre Potsdam, German Research Centre for Geosciences (GFZ), Potsdam, Germany

Abstract Waterfalls are ubiquitous, and their upstream propagation can set the pace of landscape evolution, yet no experimental studies have examined waterfall plunge pool erosion in homogeneous rock. We performed laboratory experiments, using synthetic foam as a bedrock simulant, to produce self-formed waterfall plunge pools via particle impact abrasion. Plunge pool vertical incision exceeded lateral erosion by approximately tenfold until pools deepened to the point that the supplied sediment could not be evacuated and deposition armored the pool bedrock floor. Lateral erosion of plunge pool sidewalls continued after sediment deposition, but primarily at the downstream pool wall, which might lead to undermining of the plunge pool lip, sediment evacuation, and continued vertical pool floor incision in natural streams. Undercutting of the upstream pool wall was absent, and our results suggest that vertical drilling of successive plunge pools is a more efficient waterfall retreat mechanism than the classic model of headwall undercutting and collapse in homogeneous rock.

1. Introduction

Fluvial erosion into bedrock shapes landscapes, sets downstream sediment fluxes, and imprints changes in climate and tectonics in landscape topography. In upland terrain, significant erosion can occur at waterfalls, causing waterfalls to propagate, or retreat, upstream, and waterfall retreat can be the dominant mechanism of fluvial bedrock incision [e.g., *Gilbert*, 1907; *Hayakawa et al.*, 2008; *Mackey et al.*, 2014]. Waterfall retreat requires transport of sediment away from the waterfall base to prevent headwall buttressing such that actively retreating waterfalls often have exposed bedrock at their base where plunge pools develop (Figure 1), and heightened erosion within pools can drive waterfall retreat [*Gilbert*, 1890; *Howard et al.*, 1994].

We focus on plunge pool erosion, rather than erosion of waterfall faces, because water accelerates to Froude critical or supercritical conditions at the waterfall brink [*Rouse*, 1936; 1937; *Haviv et al.*, 2006] and can detach from the waterfall face at high discharge, limiting sediment impacts on the face. The classic waterfall erosion model [*Gilbert*, 1890] invokes retreat via plunge pool undercutting of the waterfall headwall to produce a cantilever caprock that eventually collapses under its own weight. While this mechanism has been documented in flume experiments eroding horizontally stratified sediments [*Holland and Pickup*, 1976; *Frankel et al.*, 2007] and appears to hold at the type location where it was defined [*Philbrick*, 1974; *Hayakawa and Matsukura*, 2010], many waterfalls, especially those in homogeneous rock, lack evidence for headwall undercutting (Figure 1) [*Howard et al.*, 1994]. An alternative waterfall retreat mechanism is through vertical drilling of successive plunge pools leading to overall upstream retreat of a waterfall escarpment [*Howard et al.*, 1994; *Lamb et al.*, 2007]. Determining conditions for vertical drilling versus headwall undercutting are needed to build quantitative waterfall retreat models and predict landscape evolution.

Existing plunge pool erosion studies have focused on clear water scour of loose or weakly consolidated sediment [*Holland and Pickup*, 1976; *Stein et al.*, 1993] and blocks [*Bollaert and Schleiss*, 2003], which are difficult to apply to massive rock (Figure 1) where sediment impacts likely dominate erosion. Studies examining bedrock waterfall retreat have largely focused on jointed or fractured rock where retreat occurs via toppling of bedrock columns at the waterfall brink [e.g., *Weissel and Seidl*, 1997; *Lamb and Dietrich*, 2009; *Baynes et al.*, 2015; *Lapotre et al.*, 2016]. *Lamb et al.* [2007] proposed a model for vertical plunge pool abrasion by sediment impacts; however, the model has yet to be tested and makes no predictions of lateral erosion. Waterfall plunge pools share some similarities with fluvial potholes [*Elston*, 1918; *Alexander*, 1932; *Johnson and Whipple*, 2007], but the hydrodynamics of a near-vertical waterfall jet is unique for plunge pools. There exist no experimental studies, to our knowledge, of plunge pool formation in homogeneous rock via sediment abrasion. This represents a major knowledge gap which limits our ability to develop models for plunge pool erosion, waterfall retreat, and the response of landscapes to external forcing. Here we propose a conceptual

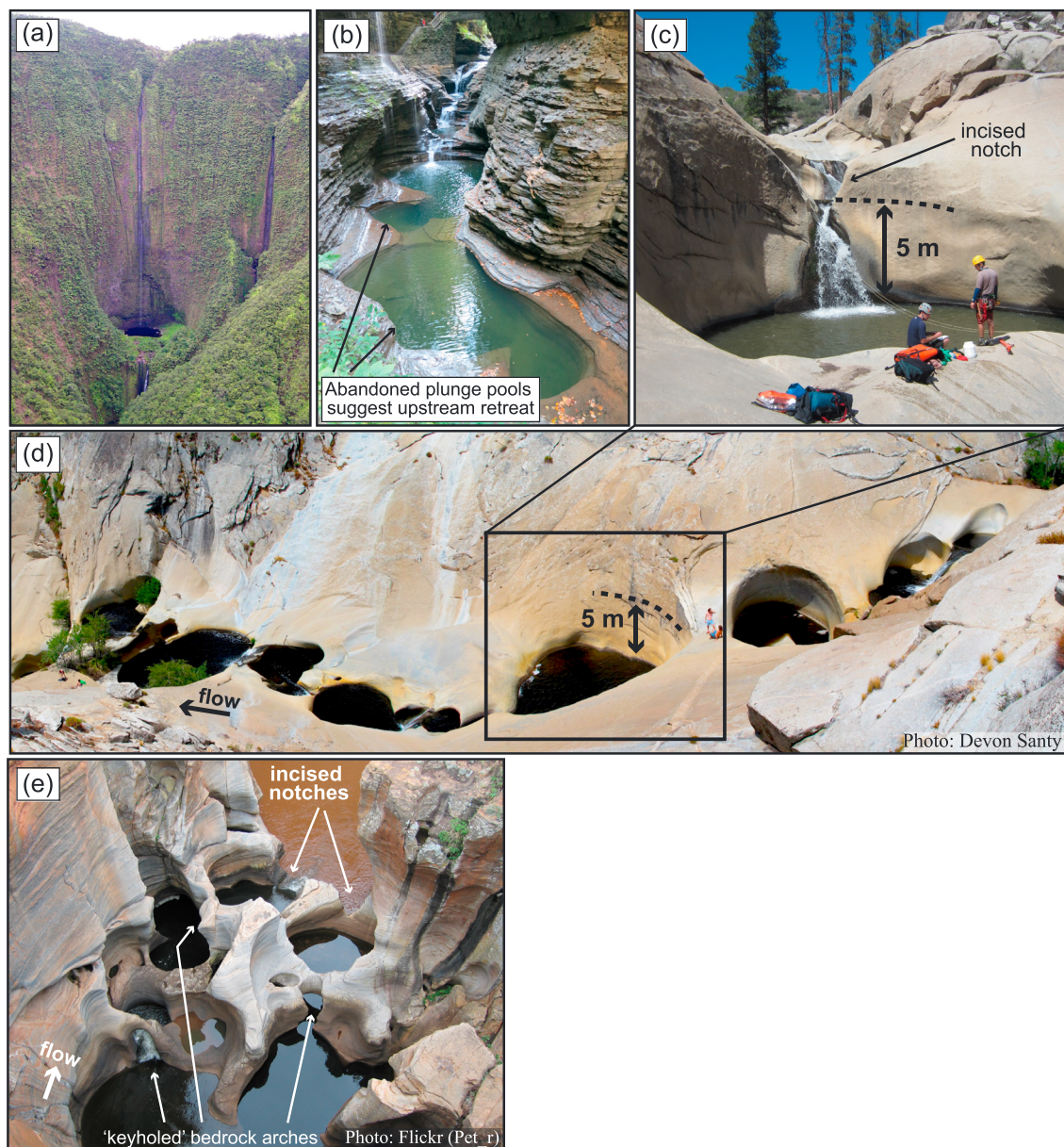


Figure 1. Waterfall plunge pools. (a) Honokāne, Hawaii, ~300 m of relief shown in image. (b) Watkins Glen, NY, channel is ~8 m wide. (c, d) Dry Meadow Creek, California. (e) Bourke's Luck Potholes, South Africa, ~20 m of relief shown in image, released under CC-BY-NC-SA-2.0. Photo in Figure 1(c) is courtesy of R. DiBiase.

model for plunge pool evolution by abrasion, which we test with laboratory experiments, and discuss implications of our results for controls on waterfall retreat.

2. Conceptual Model

Plunge pool abrasion rates likely depend on sediment impacts and the degree of sediment deposition that can protect bedrock from erosion, similar to models for vertical incision of river beds [Sklar and Dietrich, 2001; Lamb et al., 2007]. We envision that plunge pools form rapidly below bedrock steps as vertically oriented, sediment-laden waterfall jets scour sediment from the base of the step and impacting particles abrade bedrock (Figure 2a) [Elston, 1917; Howard et al., 1994; Lamb et al., 2007]. Dominance of waterfall retreat via undercutting versus vertical drilling will depend on rates of plunge pool vertical erosion relative to lateral erosion of the upstream pool wall (Figure 2a). With all else constant, vertical erosion rates should

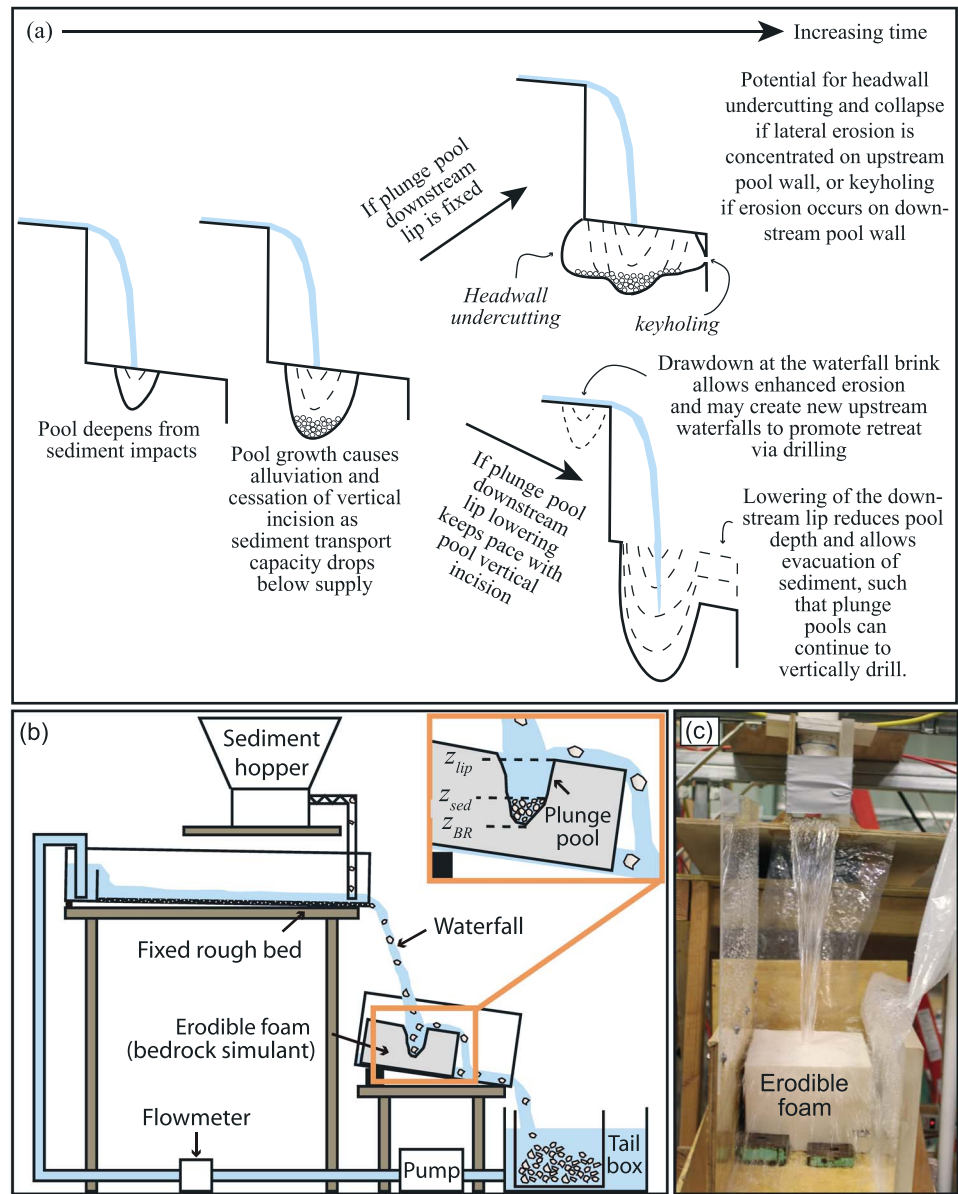


Figure 2. (a) Conceptual models for plunge pool evolution and retreat. (b) Experimental setup (adapted from Scheingross and Lamb [2016]); z_{BR} , z_{sed} , and z_{lip} are the plunge pool bedrock floor, alluvial floor, and downstream bedrock lip elevations, respectively. (c) Photograph of Exp1.

decrease with increasing pool depth as particle impact velocities slow. As plunge pools deepen, the plunge pool sediment transport capacity is reduced [Scheingross and Lamb, 2016], until eventually sediment supply exceeds transport capacity and deposition over the bedrock pool floor inhibits further vertical incision, similar to previous suggestions for plunge pools [Lamb et al., 2007] and fluvial potholes [Elston, 1918; Alexander, 1932].

Once alluviated, abrasion may still drive the lateral erosion of the pool bedrock walls, similar to widening of bedrock river channels [e.g., Finnegan et al., 2007], such that pools may experience lateral undercutting of the upstream pool wall, headwall collapse, and upstream waterfall retreat, as envisioned by Gilbert [1890] (Figure 2a). Alternatively, lateral erosion at the downstream pool wall might lead to undercutting of the pool lip, formation of a “keyhole” (Figure 1e), sediment evacuation from the pool, and continued vertical incision [Cleland, 1910; Elston, 1917]. Another possibility is that vertical erosion of the downstream pool lip keeps pace

with lowering of the bedrock pool floor; then pool depths remain shallow, sediment transport capacity exceeds sediment supply, and vertical pool erosion continues, as envisioned for vertical drilling models [Howard *et al.*, 1994; Lamb *et al.*, 2007] (Figure 2a). Thus, the mechanism of upstream waterfall retreat (i.e., headwall undercutting versus vertical drilling) should depend on the relative rates of lateral and vertical plunge pool erosion, as well as whether lateral erosion is focused on the upstream pool wall leading to headwall retreat or the downstream pool wall leading to sediment evacuation that allows continued vertical incision. Retreat via drilling also requires a mechanism to continually generate new waterfalls in the high Froude number, drawdown region at the upstream end of the escarpment [Lamb *et al.*, 2007] (Figure 2a), which might occur by morphodynamic instabilities similar to cyclic steps [Brooks, 2001; Johnson and Whipple, 2007; Yokokawa *et al.*, 2013; Izumi *et al.*, 2016].

3. Experimental Setup and Methods

In our experiments, a sediment-laden waterfall eroded plunge pools into initially planar beds under constant forcing, such that pool geometry evolved through interactions between flow hydraulics, sediment transport, and bedrock erosion (Figure 2b). Flow at the waterfall brink was supercritical (Froude numbers of ~ 1.3) and fully turbulent (Reynolds numbers of ~ 6000 and particle Reynolds numbers of ~ 160 and 460). Flow hydraulics and sediment transport in the experiments should have dynamics similar to natural plunge pools due to strong overlap in the nondimensional parameters that were found to govern plunge pool sediment transport [Scheingross and Lamb, 2016] (Figure S1 in the supporting information).

All experiments used homogeneous, polyurethane foam as a bedrock simulant, which allows for faster erosion rates at reduced scale. The foam follows the tensile strength versus erosion rate scaling as observed in natural rock, $E \propto \sigma_t^{-2}$ where E is erosion rate and σ_t is rock tensile strength [Sklar and Dietrich, 2001; Scheingross *et al.*, 2014; Lamb *et al.*, 2015], suggesting that it is a good analog for bedrock abrasion dynamics and that results can be scaled to other rock types.

Two separate experiments were carried out where a fully ventilated waterfall cascaded off an upstream channel to impact a foam block below (Table S1 and Figure 2c). Experiment 1 (Exp1) used 2.4 mm diameter, well-sorted, subrounded, natural gravel fed from a sediment feeder into the upstream river at a constant sediment flux ($Q_s = 9$ g/s), and a pump provided a constant water discharge ($Q_w = 0.58$ L/s). Experiment 2 (Exp2) used coarser 7 mm diameter, subangular grains, and, for the first 14.8 h, used identical water discharge and sediment flux to Exp1, thus isolating the effect of grain size on pool erosion. At 14.8 h in Exp2, the jet eroded through the foam block partially exposing the nonerodible floor, and consequently for the remainder of the experiment, we increased sediment flux to $Q_s = 45$ g/s, while holding water discharge and sediment size constant, to force alluviation and isolate the role of sediment supply on lateral erosion. Exp1 and Exp2 had $\sim 20\%$ differences in waterfall drop height (Table S1), resulting in 12% differences waterfall jet velocities at the plunge pool water surface [Scheingross and Lamb, 2016]. This increase is small compared to the effect of changing grain size on plunge pool sediment transport capacity; the finer grains in Exp1 are predicted to have tenfold to 500-fold higher sediment transport capacity than in Exp2 [Scheingross and Lamb, 2016]. As such, we attribute major differences in plunge pool erosion rates to reflect differences in grain size and sediment supply rather than waterfall height.

The experiments were paused periodically to measure plunge pool bedrock topography with repeat laser scans. We quantified the elevations of the downstream plunge pool lip (z_{lip}) and the lowest point on the pool floor (z_{BR}) and defined the pool depth to bedrock as the vertical distance between these points ($h_{BR} = z_{lip} - z_{BR}$) (Figure 2b). The blocks were tilted slightly in the downstream direction to ensure that sediment transported out of the plunge pool was immediately washed away. The experiments were designed to minimize erosion of the downstream plunge pool lip, and the lip was protected when detectable erosion occurred. This ensured that pools eventually deepened until the point of sediment deposition and allowed for periods when pool erosion was dominated by vertical drilling (prior to the onset of alluviation) or lateral erosion (after alluviation). Topography was scanned with a FARO-3D and an E-Scan in Exp1 and Exp2, respectively, producing millimeter to submillimeter resolution depending on the geometry. The plunge pool cross-stream width and along-stream length were measured at the elevation of z_{lip} with a ruler, and the average of the two measurements is reported as the pool radius at z_{lip} , denoted r_{pool_lip} . Because scanning did not capture undercut portions of the plunge pool, we measured the total pool volume, V_{pool} , by weighing the mass

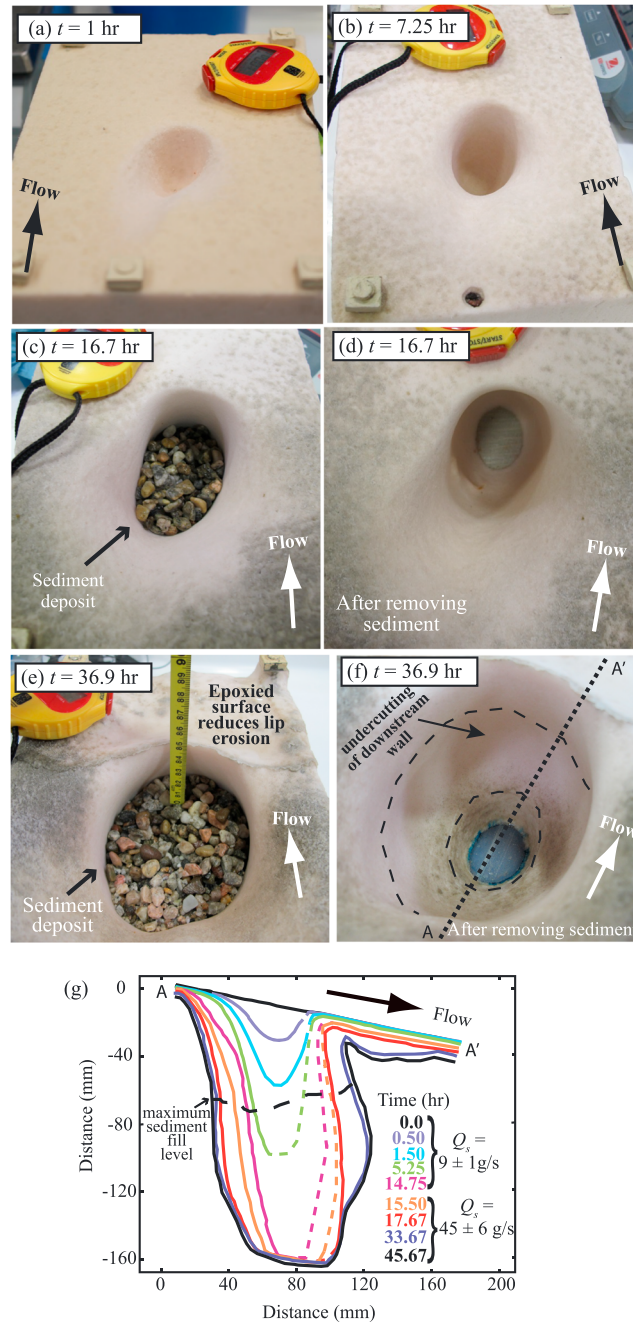


Figure 3. Progressive erosion in Exp2. (a and b) Pool morphology prior to alluviation. (c and e) Pools with deposited sediment, and (d and f) after manual sediment removal. Erosion of pool through foam bottom (which occurred at $t = 14.8$ h) is visible in Figures 3d and 3f. (g) Long profiles from laser scans showing pool evolution and sediment deposition during Exp2. Dashed lines show visual interpolation for cases when overhangs limited laser scanner line of sight. Profiles are composites merged from multiple scans using CloudCompare (<http://www.danielgm.net/cc/>).

identical to Exp1 showed no erosion after 24 h, in contrast to visible erosion in Exp1 and Exp2 within minutes of initiating sediment impacts (Figures 3 and 4).

Exp1 and Exp2 showed initially rapid vertical erosion rates (order ~ 0.1 m/h) which decreased with time to as low as $\sim 10^{-3}$ m/h as pools approached their maximum depths (Figure 4). Both experiments developed an

of water needed to fill the pool to the point of overspill while the block was laid flat. The pool volume was used to back calculate a depth-averaged plunge pool radius, $r_{\text{pool_avg}}$, assuming a cylindrical pool geometry ($r_{\text{pool_avg}} = \sqrt{V_{\text{pool}} / [\pi h_{\text{BR}}]}$). We made no volume measurements for the first 16 h of Exp1 and instead estimate $r_{\text{pool_avg}}$ using a shape factor, S_f (i.e., $r_{\text{pool_avg}} = r_{\text{pool_lip}} / S_f$). Paired measurements of $r_{\text{pool_lip}}$ and $r_{\text{pool_avg}}$ give a mean S_f of 1.38 (Table S2). Differencing successive measurements of plunge pool depth, Δh_{BR} , and average pool radius, $\Delta r_{\text{pool_avg}}$, yields the average vertical ($E_{\text{vert}} = \Delta h_{\text{BR}} / \Delta t$) and lateral ($E_{\text{lat}} = \Delta r_{\text{pool_avg}} / \Delta t$) erosion rates.

The depth to the sediment bed was measured as $h_{\text{sed}} = z_{\text{lip}} - z_{\text{sed}}$ with a ruler, where z_{sed} is the elevation of the pool alluvial floor (Figure 2b). These measurements slightly underestimate h_{sed} due to inclusion of sediment which falls out of suspension when pausing the experiment. The underlying bedrock geometry was measured by temporarily removing deposited sediment to scan the bedrock.

4. Experimental Results

Erosion occurred exclusively via abrasion from sediment impacts. Both experiments showed similar evolution where a sediment-laden waterfall jet impacted an initially flat surface, which rapidly developed a bedrock plunge pool that eventually partially filled with sediment (Figures 3 and 4 and Table S2). A preliminary clear water experiment with conditions

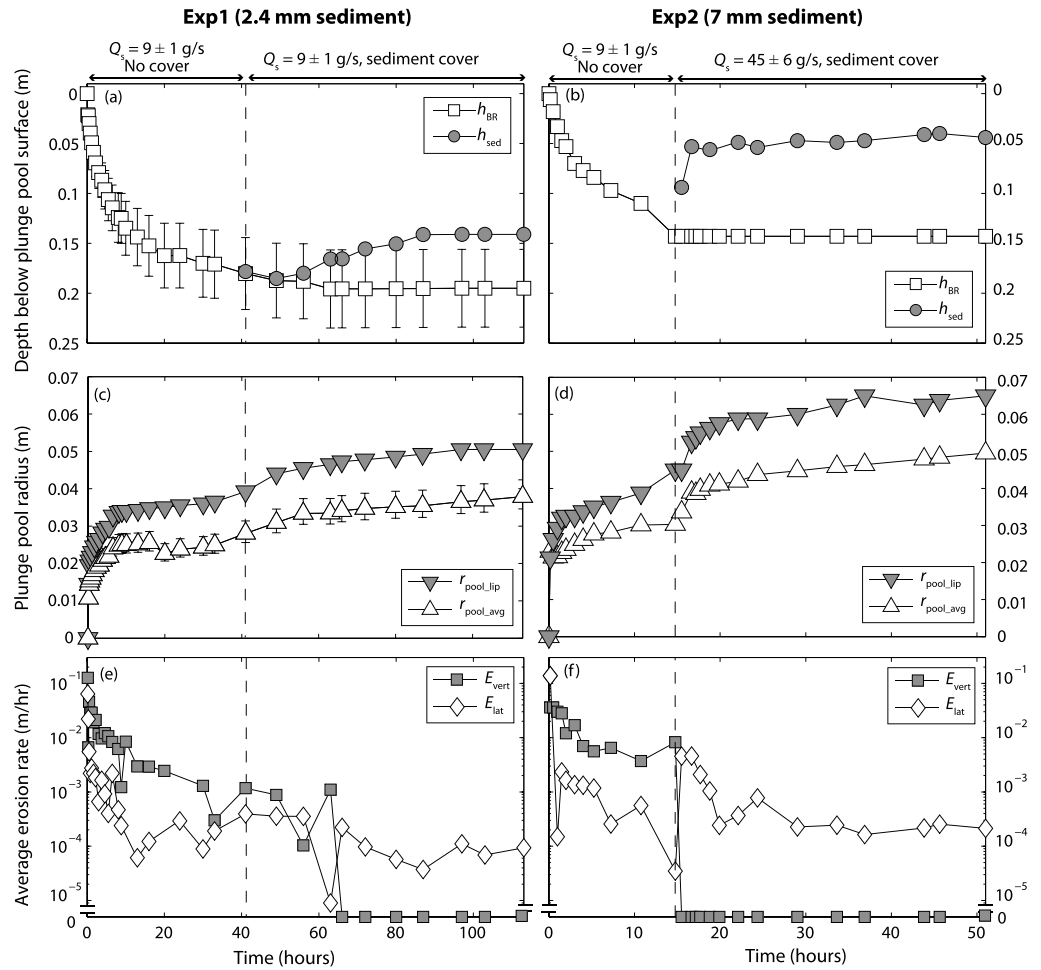


Figure 4. Evolution of plunge pools in Exp1 and Exp2. (a and b) Depth to bedrock (h_{br}) and sediment (h_{sed}); h_{sed} is not shown when $h_{sed} = h_{br}$. (c and d) Average plunge pool radius measured at the pool lip (r_{pool_lip}) and back calculated from pool volume (r_{pool_avg}). (e and f) Average vertical (E_{vert}) and lateral (E_{lat}) plunge pool erosion rates. Broken y axis shows cases of zero erosion. Dashed lines denote sediment cover onset. Error bars represent error associated with FARO-3D scanner for deep and narrow pools.

alluvial cover over the pool bedrock floor as sediment supply exceeded transport capacity; this occurred in Exp1 due to internal dynamics as the pool eroded deeper, and it was imposed in Exp2 by the fivefold increase in sediment flux at $t = 14.8$ h (Figure 4). In Exp1 sediment began to deposit on the pool floor at $t = 41$ h (Table S2); however, vertical plunge pool erosion continued from $t = 41$ – 63 h. This suggests active interchange of the deposited and mobile sediment (i.e., it represents an “active layer” that is common in gravel bed rivers [Parker, 2008]) so that despite the occurrence of a sediment deposit, grains continued to impact the bedrock during the interchange process resulting in bedrock erosion (Figure 4e). At $t = 63$ h the sediment bed thickness increased to >10 grain diameters and vertical incision ceased, suggesting that a static layer of grains formed that protected the bedrock from erosion (Figure 4a). Similar observations were made in Exp2 where a sediment deposit, ~ 7 grain layers thick, formed at $t = 14.8$ h and grew to ~ 15 grain layers by the end of the experiment (Figure 4b and Table S2). At $t = 43.8$ h we carefully removed, spray painted, and returned grains to the pool and found at $t = 45.7$ h that spray-painted particles up to ~ 10 grain diameters below z_{sed} were replaced by paint-free grains, while deeper grains remained in place, suggesting the presence of an active layer overlying a static deposit below.

Both experiments had initially high lateral erosion rates which decreased with time until sediment was deposited on the pool floor. After alluviation, lateral erosion rates briefly spiked and then declined to near-constant values (Figure 4). Prior to sediment deposition, the pools primarily eroded vertically with little

change in radius. Scans in Exp2 show that immediately after sediment deposition ($t = 14.8$ to 17.7 h), lateral erosion occurred throughout the pool resulting in approximately parallel wall retreat for both upstream and downstream walls (Figure 3g). However, after $t = 17.7$ h lateral erosion was reduced at the upstream pool wall and instead was focused at the downstream wall within the active layer. The only undercutting that occurred in the experiment was of the downstream pool wall (Figure 3g).

Comparing Exp1 and the first 14.8 h of Exp2 allows examination of the influence of grain size because Exp1 used approximately threefold finer sediment than Exp2. Plunge pool radii were typically $\sim 30\%$ greater in Exp2, possibly due to the coarser sediment. However, there are no major differences in plunge pool vertical or lateral erosion rates between the two experiments (Figure 4). This suggests that when sediment supply is less than transport capacity, erosion rates are more strongly tied to sediment supply than particle size.

5. Discussion

5.1. Controls on Vertical and Lateral Plunge Pool Erosion

The experiments support the conceptual model in which pools initially rapidly erode and morphodynamic feedbacks lead to deposition, forcing vertical erosion to cease, while lateral erosion continues. We attribute the initially high vertical erosion rates to energetic particle impacts, in which fluid drag in shallow pools is not sufficient to slow impact velocities. As pools deepen, vertical erosion likely slows as fluid drag within the pool reduces particle impact velocities [Lamb *et al.*, 2007], and because the pool sediment transport capacity decreases [Scheingross and Lamb, 2016], such that patchy sediment cover can reduce erosion rates [e.g., Sklar and Dietrich, 2004; Lamb *et al.*, 2007].

The initially rapid lateral erosion rates in the experiments (Figures 4e and 4f) likely come from pool width adjustment to match the size of the impinging waterfall jet. Particles falling from the waterfall brink are entrained within the waterfall jet, which expands within the plunge pool [e.g., Rajaratnam, 1976; Scheingross and Lamb, 2016]. The initial rapid increase in plunge pool radius may occur from subvertically directed impacts of particles entrained within the descending jet. Once pools grow much wider than the plunge pool jet, particles with subvertical trajectories no longer hit the pool walls, and lateral erosion must instead be driven by horizontally directed impacts from particles entrained within the pool. These impacts are probably less energetic than impacts from grains falling from the waterfall brink, which may explain the sharp decreases in lateral erosion observed after $t \sim 5$ h in our experiments (Figure 4).

Continued pool deepening and widening, with z_{lip} and all else held constant in our experiments, eventually led to sediment supply in excess of plunge pool sediment transport capacity, the onset of alluviation, and the cessation of vertical erosion (Figure 4). We interpret the spike in plunge pool lateral erosion rates after the onset of alluviation in our experiments to result from an increase in the rate of particle-wall impacts associated with the increase in near-wall sediment concentration as the pool transitions from a sparsely covered bedrock floor to a fully alluviated floor. The fact that this spike is greater in Exp2 than Exp1 is consistent with this hypothesis due to the fivefold increase in sediment supply imposed in Exp2. We find that vertical erosion can continue through particle interchange in an active layer, until the deposit is greater than ~ 10 grain diameters thick. At this point a static layer of grains develops at the bedrock-sediment interface, and vertical bedrock erosion ceases. Lateral erosion continues on the exposed bedrock walls but surprisingly is focused on the downstream pool wall. Lateral erosion causes further pool widening, which decreases the plunge pool sediment transport capacity [Scheingross and Lamb, 2016] and leads to continued sediment aggradation.

5.2. Implications for Plunge Pool Undercutting Versus Drilling

Plunge pool undercutting and headwall collapse is commonly cited as a dominant waterfall retreat mechanism [e.g., Gilbert, 1890; Anderson and Anderson, 2010]. However, many waterfalls show no undercutting (Figure 1), and we did not observe undercutting of the upstream pool wall in our experiments. Undercutting that did occur was focused on the downstream pool wall. In addition, in both experiments, the rates of vertical incision outpaced lateral erosion on average by a factor of ~ 10 , until the pool developed a static sediment layer on the bed (Figure 4 and Table S2). Moreover, even after vertical incision ceased, lateral erosion rates were small and decreased as the pool widened relative to the jet radius. These results imply that undercutting in homogenous rock, if it occurs, is an inefficient waterfall retreat mechanism. For example, we expect fluvial bedrock erosion rates upstream of the waterfall, scaled for our experiments, to outpace

undercutting after pool alluviation by a factor of ~5 and 13 in Exp1 and Exp2, respectively (Text S1), implying that waterfalls limited to undercutting in homogeneous rock may be unstable and rapidly shrink in height.

These results point to the importance of layered rock of varying strength in promoting upstream headwall undercutting and retreat, as classically envisioned [Gilbert, 1890]. For example, overcoming a tenfold difference between upstream fluvial erosion rates relative to lateral plunge pool erosion, similar to observations in our experiments, requires an approximately threefold difference in tensile strength between rock layers assuming $E \propto \sigma_t^{-2}$ [Sklar and Dietrich, 2001], which is reasonable given the range of tensile strengths of common rock types. However, as pools undercut headwalls to larger distances, lateral erosion rates should decrease further owing to reduced particle velocities in larger plunge pools [Scheingross and Lamb, 2016], such that retreat via undercutting will be most effective for caprocks that can fail with minimal undercut distances.

In the absence of undercutting, we argue that waterfall retreat in homogeneous rock is likely driven by vertical drilling of successive plunge pools [Howard et al., 1994; Lamb et al., 2007]. Sustained retreat of this form requires plunge pool vertical incision to outpace lateral plunge pool erosion and upstream fluvial incision, consistent with our experimental observations where plunge pool vertical incision outpaced lateral erosion (and inferred upstream fluvial incision; Text S1) by an average of approximately tenfold up until the point of pool alluviation (Figure 4 and Table S2). In natural pools, erosion of the downstream pool lip should decrease pool depths, limiting alluviation and allowing pools to persistently scour the bedrock pool floor. Although pool lip erosion was purposefully limited in our experiments to isolate controlling variables, natural plunge pools frequently display incised notches at their downstream lips (Figure 1), suggesting a coevolution of plunge pool floors and lips. Additionally, waterfalls formed in homogeneous rock tend to occur in series (Figure 1) [Lamb et al., 2007; DiBiase et al., 2015] such that focused lateral erosion of the downstream plunge pool wall after alluviation, as we observed in the experiments (Figure 3g), might produce keyholes where erosion through the pool wall creates a hole in the downstream waterfall face leaving behind a bedrock arch (Figure 1e) [Cleland, 1910; Elston, 1917]. Keyholes provide a path to flush sediment out of pools enabling continued vertical incision of the pool floor. In turn, new pools might be generated through cyclic-step or step-pool morphodynamics in the supercritical drawdown region upstream of the waterfall brink (Figure 2a) [Johnson and Whipple, 2007; Yokokawa et al., 2013; Scheingross, 2016; Izumi et al., 2016].

6. Conclusions

Experimental plunge pools in a homogeneous bedrock simulant evolved via initially rapid rates of vertical and lateral incision, which slowed as pools deepened. When sediment transport capacity dropped below sediment supply, deposition on the pool floor limited further vertical incision. While waterfall retreat is classically assumed to occur via plunge pool undercutting of the upstream headwall, our experiments instead show focused erosion at the downstream pool wall, which could lead to the formation of keyholes that allow sediment evacuation and continued vertical erosion. Moreover, vertical plunge pool incision rates outpaced lateral erosion rates by an average of approximately tenfold until the onset of sediment deposition. We suggest that waterfall escarpment retreat in homogeneous rock is dominated by vertical plunge pool drilling, facilitated by undercutting or vertical lowering of the downstream plunge pool lip, rather than the classic model of headwall undercutting and collapse.

Acknowledgments

Experimental data are tabulated in the supporting information; additional data are available from J.S.S. Brian Fuller and Conor O'Toole assisted with experiments. We thank Jeff Prancevic, Roman DiBiase, Florent Gimbert, and Jens Turowski for discussion and Edwin Baynes and an anonymous reviewer for constructive comments. We acknowledge National Science Foundation funding via EAR-1147381 to M.P.L. and a Graduate Research Fellowship to J.S.S., NASA funding via 12PGG120107 to M.P.L., and an Alexander von Humboldt Fellowship to J.S.S. The Caltech Summer Undergraduate Research Fellowship program partially supported D.Y.L.

References

- Alexander, H. (1932), Pothole erosion, *J. Geol.*, 40(4), 305–337.
- Anderson, R. S., and S. P. Anderson (2010), *Geomorphology: The Mechanics and Chemistry of Landscapes*, Cambridge Univ. Press, Cambridge, doi: 10.1111/j.1745-7939.2012.01222_5.x.
- Baynes, E. R. C., M. Attal, S. Niedermann, L. A. Kirstein, A. J. Dugmore, and M. Naylor (2015), Erosion during extreme flood events dominates Holocene canyon evolution in northeast Iceland, *Proc. Natl. Acad. Sci. U.S.A.*, 112(8), 2355–2360, doi:10.1073/pnas.1415443112.
- Bollaert, E., and A. Schleiss (2003), Scour of rock due to the impact of plunging high velocity jets. Part I: A state-of-the-art review, *J. Hydraul. Res.*, 41(5), 451–464, doi:10.1080/00221680309499991.
- Brooks, P. C. (2001), *Experimental Study of Erosional Cyclic Steps*, Univ. of Minnesota, Minnesota.
- Cleland, H. F. (1910), North American natural bridges, with a discussion of their origin, *Geol. Soc. Am. Bull.*, 21(1), 313–338, doi:10.1130/GSAB-21-313.
- DiBiase, R. A., K. X. Whipple, M. P. Lamb, and A. M. Heimsath (2015), The role of waterfalls and knickzones in controlling the style and pace of landscape adjustment in the western San Gabriel Mountains, California, *Geol. Soc. Am. Bull.*, 127(3–4), 539–559, doi:10.1130/B31113.1.
- Elston, E. D. (1917), Potholes: Their variety, origin and significance, *Sci. Mon.*, 5(6), 554–567.

- Elston, E. D. (1918), Potholes: Their variety, origin and significance. II, *Sci. Mon.*, 6(1), 37–51.
- Finnegan, N. J., L. S. Sklar, and T. K. Fuller (2007), Interplay of sediment supply, river incision, and channel morphology revealed by the transient evolution of an experimental bedrock channel, *J. Geophys. Res.*, 112, F03S11, doi:10.1029/2006JF000569.
- Frankel, K. L., F. J. Pazzaglia, and J. D. Vaughn (2007), Knickpoint evolution in a vertically bedded substrate, upstream-dipping terraces, and Atlantic slope bedrock channels, *Geol. Soc. Am. Bull.*, 119(3–4), 476–486, doi:10.1130/b25965.1.
- Gilbert, G. K. (1890), The history of the Niagara River, extracted from the sixth annual report to the commissioners of the state reservation at Niagara, Albany, N. Y.
- Gilbert, G. K. (1907), The rate of recession of Niagara Falls, *US Geol. Surv. Bull.*, 306, 1–31.
- Haviv, I., Y. Enzel, K. X. Whipple, E. Zilberman, J. Stone, A. Matmon, and L. K. Fifield (2006), Amplified erosion above waterfalls and over-steepened bedrock reaches, *J. Geophys. Res.*, 111, F04004, doi:10.1029/2006JF000461.
- Hayakawa, Y. S., and Y. Matsukura (2010), Stability analysis of waterfall cliff face at Niagara Falls: An implication to erosional mechanism of waterfall, *Eng. Geol.*, 116(1–2), 178–183, doi:10.1016/j.enggeo.2010.08.004.
- Hayakawa, Y. S., S. Yokoyama, and Y. Matsukura (2008), Erosion rates of waterfalls in post-volcanic fluvial systems around Aso volcano, southwestern Japan, *Earth Surf. Process. Landf.*, 33(5), 801–812, doi:10.1002/esp.1615.
- Holland, W. N., and G. Pickup (1976), Flume study of knickpoint development in stratified sediment, *Geol. Soc. Am. Bull.*, 87(1), 76–82, doi:10.1130/0016-7606(1976)87<76:fsokdi>2.0.co;2.
- Howard, A. D., W. E. Dietrich, and M. A. Seidl (1994), Modeling fluvial erosion on regional to continental scales, *J. Geophys. Res.*, 99(B7), 13,971–13,986, doi:10.1029/94JB00744.
- Izumi, N., M. Yokokawa, and G. Parker (2016), Incisional cyclic steps of permanent form in mixed-bedrock-alluvial rivers, *J. Geophys. Res. Earth Surf.*, 121, doi:10.1002/2016JF003847.
- Johnson, J. P., and K. X. Whipple (2007), Feedbacks between erosion and sediment transport in experimental bedrock channels, *Earth Surf. Process. Landf.*, 32(7), 1048–1062, doi:10.1002/esp.1471.
- Lamb, M. P., and W. E. Dietrich (2009), The persistence of waterfalls in fractured rock, *Geol. Soc. Am. Bull.*, 121(7–8), 1123–1134, doi:10.1130/b26482.1.
- Lamb, M. P., A. D. Howard, W. E. Dietrich, and J. T. Perron (2007), Formation of amphitheater-headed valleys by waterfall erosion after large-scale slumping on Hawai'i, *Geol. Soc. Am. Bull.*, 119(7–8), 805–822, doi:10.1130/b25986.1.
- Lamb, M. P., W. E. Dietrich, and L. S. Sklar (2008), A model for fluvial bedrock incision by impacting suspended and bed load sediment, *J. Geophys. Res.*, 113, F03025, doi:10.1029/2007JF000915.
- Lamb, M. P., N. J. Finnegan, J. S. Scheingross, and L. S. Sklar (2015), New insights into the mechanics of fluvial bedrock erosion through flume experiments and theory, *Geomorphology*, 244, 33–55, doi:10.1016/j.geomorph.2015.03.003.
- Lapotre, M. G. A., M. P. Lamb, and R. M. E. Williams (2016), Canyon formation constraints on the discharge of catastrophic outburst floods of Earth and Mars, *J. Geophys. Res. Earth Surf.*, 121, 1232–1263, doi:10.1002/2016JE005061.
- Mackey, B. H., J. S. Scheingross, M. P. Lamb, and K. A. Farley (2014), Knickpoint formation, rapid propagation, and landscape response following coastal cliff retreat at the last interglacial sea-level highstand: Kaua'i, Hawai'i, *Geol. Soc. Am. Bull.*, 126(7–8), 925–942, doi:10.1130/b30930.1.
- Parker, G. (2008), Transport of gravel and sediment mixtures, in *Sedimentation Engineering: Processes, Measurements, Modeling, and Practice*, edited by M. H. Garcia, American Society of Civil Engineers, Reston, Virginia, doi:10.1061/9780784408148.
- Philbrick, S. S. (1974), What future for Niagara Falls, *Geol. Soc. Am. Bull.*, 85(1), 91–98, doi:10.1130/0016-7606(1974)85<91:Wffnf>2.0.Co;2.
- Rajaratnam, N. (1976), *Turbulent Jets*, Elsevier, Amsterdam.
- Rouse, H. R. (1936), Discharge characteristics of the free overfall, *Civ. Eng.*, 6, 257–260.
- Rouse, H. R. (1937), Pressure distribution and acceleration at the free overfall, *Civ. Eng.*, 7, 518.
- Scheingross, J. S. (2016), *Mechanics of Sediment Transport and Bedrock Erosion in Steep Landscapes*, California Institute of Technology, Pasadena, Calif., doi:10.7907/Z9B8562B.
- Scheingross, J. S., and M. P. Lamb (2016), Sediment transport through waterfall plunge pools, *J. Geophys. Res. Earth Surf.*, 121, doi:10.1002/2015JF003620.
- Scheingross, J. S., F. Brun, D. Y. Lo, K. Omerdin, and M. P. Lamb (2014), Experimental evidence for fluvial bedrock incision by suspended and bedload sediment, *Geology*, 42(6), 523–526, doi:10.1130/G35432.1.
- Sklar, L. S., and W. E. Dietrich (2001), Sediment and rock strength controls on river incision into bedrock, *Geology*, 29(12), 1087–1090, doi:10.1130/0091-7613(2001)029<1087:sarsco>2.0.co;2.
- Sklar, L. S., and W. E. Dietrich (2004), A mechanistic model for river incision into bedrock by saltating bed load, *Water Resour. Res.*, 40(6), doi:10.1029/2003WR002496.
- Stein, O. R., C. V. Alonso, and P. Y. Julien (1993), Mechanics of jet scour downstream of a headcut, *J. Hydraul. Res.*, 31(6), 723–738, doi:10.1080/00221689309498814.
- Weissel, J. K., and M. A. Seidl (1997), Influence of rock strength properties on escarpment retreat across passive continental margins, *Geology*, 25(7), 631–634, doi:10.1130/0091-7613(1997)025<0631:iorspo>2.3.co;2.
- Yokokawa, M., A. Kotera, and A. Kyogoku (2013), Cyclic steps by bedrock incision, in *Advances in River Sediment Research*, edited by S. Fukuoka et al., CRC Press, Netherlands.